# A Photochemical Activation Scheme of Inert Dinitrogen by Dinuclear $Ru^{II}$ and $Fe^{II}$ Complexes

**Markus Reiher,*[a] Barbara Kirchner,[a] Jürg Hutter,[b] Dieter Sellmann,[c] and Bernd Artur Hess[a]**

**Abstract:** A general photochemical activation process of inert dinitrogen coordinated to two metal centers is presented on the basis of high-level DFT and ab initio calculations. The central feature of this activation process is the occupation of an antibonding π* orbital upon electronic excitation from the singlet ground state $S_0$ to the first excited singlet state $S_1$. Populating the antibonding LUMO weakens the triple bond of dinitrogen. After a vertical excitation, the excited complex may structurally relax in the $S_1$ state and approaches its minimum structure in the $S_1$ state. This excited-state minimum structure features the dinitrogen bound in a diazenoid form, which exhibits a double bond and two lone pairs localized at the two nitrogen atoms, ready to be protonated. Reduction and de-excitation then yield the corresponding diazene complex; its generation represents the essential step in a nitrogen fixation and reduction protocol. The consecutive process of excitation, protonation, and reduction may be rearranged in any experimentally appropriate order. The protons needed for the reaction from dinitrogen to diazene can be provided by the ligand sphere of the complexes, which contains sulfur atoms acting as proton acceptors. These protonated thiolate functionalities bring protons close to the dinitrogen moiety. Because protonation does not change the π*-antibonding character of the LUMO, the universal and well-directed character of the photochemical activation process makes it possible to protonate the dinitrogen complex *before* it is irradiated. The π*-antibonding LUMO plays the central role in the activation process, since the diazenoid structure was obtained by excitation from various occupied orbitals as well as by a direct two-electron reduction (without photochemical activation) of the complex; that is, the important bending of $N_2$ towards a diazenoid conformation can be achieved by populating the π*-antibonding LUMO.

**Keywords:** density functional calculations · excited state structures · iron · nitrogen fixation

## Introduction

Activation of small molecules by transition-metal complexes is a major research area in catalysis. In this context, the main purpose of a transition-metal complex is usually the *direct* activation of the small molecule through a weakening of a bond or even bond breaking upon coordination. In this work, we investigate the example of nitrogen fixation, that is, the reduction of dinitrogen to ammonia, which is still a challenge in coordination chemistry. In the case of dinitrogen reduction, the activation of $N_2$ upon coordination is usually measured in terms of bond elongation (towards diazene- or hydrazine-like N–N bond lengths) or of force constants obtained from vibrational spectroscopy (compare refs. [1,2] for recent examples and refs. [3–6] for reviews). The reduction of the $N_2H_x$ ($x=0,1,2$) species can then be achieved either by direct use of strong reductants or by the metal complexes itself (see, e.g., refs. [7–15]) into which the reductive power has been deposited on preparation of the complex. The decisive aspect for nitrogen fixation is that these systems should work catalytically.

Apart from potential "thermochemical" nitrogen activation pathways, photochemical reactions have also been discovered. For instance, Floriani et al. achieved cleavage of the N≡N triple bond via irradiation of dinuclear molybdenum based complexes, which bind $N_2$ end-on.[16] This light-assisted cleavage reaction produced presumably end-on bound monomeric nitride complexes, which then reacted

[a] Priv.-Doz. Dr. M. Reiher, Dr. B. Kirchner, Prof. Dr. B. A. Hess
Lehrstuhl für Theoretische Chemie, Universität Bonn
Wegelerstrasse 12, 53115 Bonn (Germany)
Fax: (+49) 228-73-9064
E-mail: Reiher@thch.uni-bonn.de

[b] Prof. Dr. J. Hutter
Physikalisch-chemisches Institut, Universität Zürich
Winterthurerstrasse 190, 8057 Zürich (Switzerland)

[c] Prof. Dr. D. Sellmann
Lehrstuhl für Anorganische Chemie
Universität Erlangen-Nürnberg
Egerlandstrasse 1, 91058 Erlangen (Germany)

 **DOI: 10.1002/chem.200400081**  

with the remaining reactant molecules. We should emphasize, however, that this reaction purely demonstrates the bond cleavage, but not reduction of $N_2$; it is assumed to be important in $N_2$ photoactivation research. As a second example we would like to mention the work of Kisch and coworkers who confirmed the findings of Schrauzer and Guth[17] in a recent study[18,19] that ammonia can be produced through light absorption by semiconductor powder (which was previously questioned by Edwards et al.[20,21] in view of contradictory results). In this case, the postulated photofixation mechanism, which is consistent with the experimental findings, involves the production of adsorbed hydrogen atoms from the decomposition of water, which then reduce molecular nitrogen.[18,19] The photochemical effect thus relies on the production of the strong reductant "atomic hydrogen".

The production of diazene is the thermodynamically decisive step and thus the most important step in dinitrogen reduction.[22] Once this has been accomplished, subsequent reduction or disproportionation (see ref. [23]) to hydrazine and ammonia might be possible. While the enzyme nitrogenase[4,24,25–27] processes this reduction under ambient conditions without extraordinarily strong reductants or temperature and pressure conditions, model complexes usually need strong reductants (in some way or another) and do not provide proton acceptors in their ligand spheres, which are essential for bringing protons close to the reaction center. The first catalytic dinitrogen reducing system was presented in the recent work by Yandulov and Schrock, who used a molybdenum triamidoamine complex.[28–30]

In this study, we advocate for a different protocol in dinitrogen reduction research, in which the transition-metal complex serves in the first step merely as a coordination site, which fixes $N_2$ spatially without significant activation, that is, without significant elongation of the N≡N triple bond. In a subsequent second step, the energy for the activation is then provided by irradiation of UV/Vis light, which forces the transition-metal complex in an excited state. It is most important to understand that this excited state does not represent an ill-defined storage for the photon energy, which would then result in uncontrolled reactions. Instead, the particular excited state must enable a well-directed activation of $N_2$ through excitation in an antibonding molecular orbital. This idea of utilizing π* orbitals of the $N_2$ moiety is straightforward and has therefore been suggested earlier in the literature;[31] certain bands in the electronic spectra of various dinitrogen complexes could indeed be assigned to transitions into π* orbitals (in an idealized, qualitative quantum chemical one-particle picture).[32–34] However, it is by far less clear whether the occupation of a π*-antibonding molecular orbital can then produce a diazene-like conformation with $N_2$ possessing a double bond and two lone pairs at the nitrogen atoms as depicted in Figure 1.

Once this can be achieved, such a diazenoid structure can be protonated to give diazene in a subsequent reduction step. In principle, the order of activation, reduction, and protonation might be varied as demonstrated in Figure 2 for a dinuclear dinitrogen coordinating complex. While our focus here is on analyzing the general capability of certain dinuclear metal complexes for undergoing a sequence of

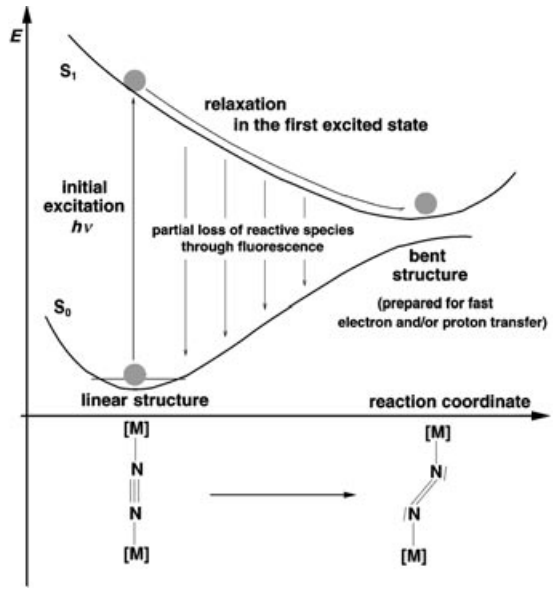


Figure 1. Schematic representation of the postulated photochemical activation scheme; various (also non-radiative) side reactions may occur, which are not shown.

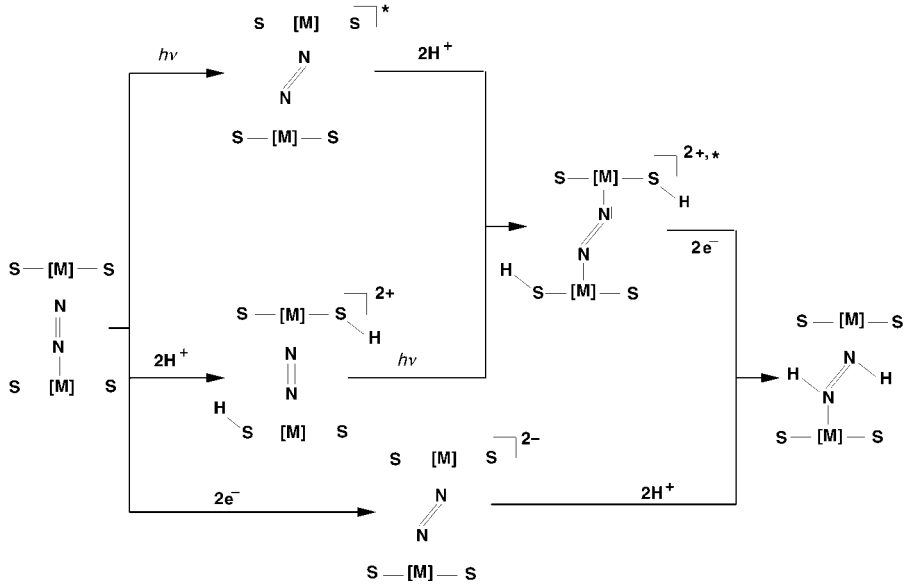


Figure 2. Hypothetical reduction process of coordinated dinitrogen through consecutive protonation, reduction, and excitation processes.

these three steps, we note that the *detailed* mechanism of reduction and protonation is not only important for the model complexes but also for the enzyme nitrogenase. The importance of understanding cooperativity effects and mechanochemical couplings of reduction and protonation in metalloenzymes has recently been stressed by Xavier et al.[35]

In this work, we study the potential photochemical activation process by employing biomimetic nitrogenase model complexes, which were synthesized by Sellmann and coworkers.[36–40] The biomimetic aspect of these systems relies on the "open-side model" introduced by Sellmann (see refs. [37,38]) and has recently been supported by first-principles calculations on the mechanism of the active center of nitrogenase, that is, of the FeMo cofactor.[41] These model complexes feature thiolate and thioether functional groups in the coordination sphere of iron and ruthenium metal centers. In this respect, they resemble parts of the structure of the FeMo-cofactor. Since it is well known that ruthenium binds unstable $N_2H_x$ species stronger than iron, which has also been confirmed for Sellmann-type complexes in quantum chemical calculations,[42] Ru complexes are often used for testing synthetic strategies, which can afterwards be tested for iron analogues. Consequently, the first (mononuclear and dinuclear) dinitrogen Sellmann-type complexes **1** were obtained recently with ruthenium as the central metal atom.[43–45] The experimentally known dinuclear dinitrogen–ruthenium complex is the starting point for our theoretical dinitrogen activation study.[44] The Lewis structures of this and an additional dinuclear Sellmann-type metal complex, which we selected in order to demonstrate the general aspects of the photochemical activation process, are depicted in Figure 3. Complexes of type **2** were obtained[46–49] as a low-spin derivative of chelate ligands with a secondary amine in *trans*-position[50] in place of the pyridine.

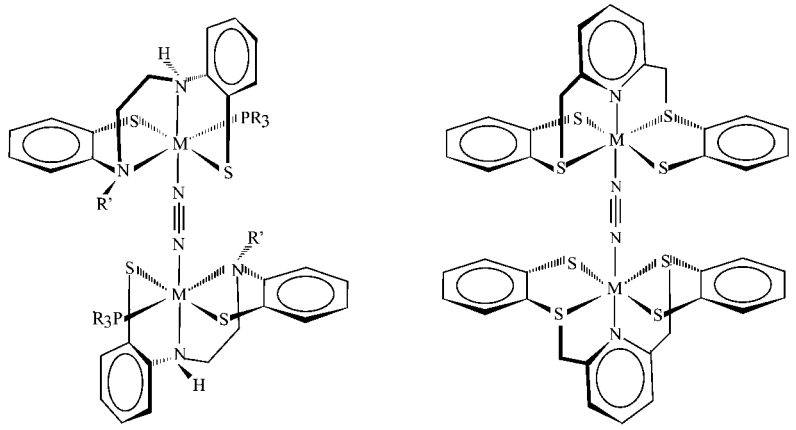


**1** **2**

Figure 3. Lewis structures of biomimetic model complexes. Left: "$S_2N_2$" complex **1** (experimentally known with R′ = Me and R = alkyl); right: "$N_{pyr}S_4$" complex **2**.

After the description of the quantum chemical methodology in the next Section, the structural and energetical features of the complexes in Figure 2 are discussed subsequently. This discussion allows us to examine the principle features of a photochemical activation pathway. A quantitative analysis of a simplified model of the experimentally known dinuclear $N_2$ complex **1** provides additional information on the details of the postulated photochemical process (Section on Quantitative Investigation). We shall demonstrate that the photochemical activation is possible for different chelate ligands and metal center atoms and is solely governed by the character of the LUMO in these complexes.

## Quantum Chemical Methodology

For all ground-state restricted Kohn–Sham calculations we applied the density functional programs provided by the Turbomole 5.1 suite.[51] For Ru we employed pseudo-potentials of the Stuttgart group[52] as implemented in Turbomole. Ahlrichs' TZVP basis set featuring a valence triple-zeta basis set with polarization functions on all atoms is used.[53] For the calculation of vertical excitation energies we applied the time-dependent BP86[54,55] and B3LYP[56,57] density functional programs of the Turbomole package.[58,59] The B3LYP functional has been employed in addition to the BP86 functional, which is known to produce accurate molecular structures for the type of complexes under consideration[42], since B3LYP excitation energies are, in general, more reliable than those from BP86 calculations.[60] In connection with the BP86 density functional calculations for the ground states we always used the resolution-of-the-identity (RI) technique.[61,62]

Moreover, these two density functionals were chosen since they are very well established representatives of pure and hybrid density functionals yielding reasonable reaction energetics in a large number of cases. However, the situation is different for iron compounds where unreliable energetics were obtained for complexes of the type under study.[42] A systematic study has shown that these iron complexes represent critical cases where high-spin-low-spin energy splittings are small and can differ largely when calculated with pure and hybrid density functionals.[63] In order to avoid these uncertainties we use in addition to BP86 and B3LYP our re-parametrized B3LYP*, which was tailored particularly for these complexes[63] but which has shown to be of general applicability.[64] For the discussion of reaction energetics we rely on the B3LYP* data and give energies for the two other density functionals only for comparison.

For the frequency analyses the program package SNF was employed.[65] The second derivatives of the total electronic

  

energy of the harmonic force field were calculated numerically from analytic energy gradients of distorted structures. Scaling factors for a re-adjustment of the calculated frequencies were not applied.

The main contribution to the excitation from $S_0 \rightarrow S_1$ turned out to be a HOMO→LUMO transition which is of charge-transfer type (from the sulfur lone-pairs to the π* orbital of the $N_2$ moiety). Such excitations are not well described by TDDFT (neither with the B3LYP nor with the BP86 functional). Therefore, we performed calculations of excitation energies with the TZVP basis set within the framework of multi-reference second-order perturbation theory (MR-MP2) with the multi-reference 2nd-order Møller-Plesset code by Grimme and Waletzke.[66]

However, a MR-MP2 program for structure optimizations with analytic gradients is not available so that we used efficient DFT and TDDFT calculations in combination with the BP86 functional for the generation of excited state minimum structures. Ground-state DFT calculations were applied for this purpose because we were able to exploit the different symmetry of HOMO and LUMO in $C_i$ point group symmetry. Occupation of the LUMO then leads to an at most semi-quantitative description of the electronic structure if we assume that the modified electronic configuration may become the ground state configuration for the diazenoid structure. A second, quantitative scheme is provided by a TDDFT optimization in the excited state. Though the excitation energy in this calculation may be non-quantitative, the change of structure of our rigid complexes can be expected to be sufficiently accurate.

For the TDDFT structure optimization in the first excited singlet state $S_1$ we applied the recent development of *analytic* excited state energy gradients in the CPMD code[68] within the Tamm–Dancoff approximation.[67] Troullier–Martins norm-conserving pseudo potentials[69] with a 70 Ryd cutoff were used. For all atoms excluding ruthenium we chose the electron configuration of the neutral atomic ground state for the generation of the pseudo potentials. Ruthenium was treated as an ionic system in the $Ru^{III}$ configuration (atomic spectroscopy notation), that is, $Ru^{2+}$ with electronic configuration ($4d^6$). The 4s and 4p semi-core one-electron states were included explicitly in the calculation. The core radii ($r_c$ in atomic units) were 1.2 for carbon, 1.12 for nitrogen, 1.5 for phosphorus, 1.4 for sulfur, and 0.5 for hydrogen. The same values for all angular momentum states were employed. The $r_c$ values for ruthenium were 1.1 (l=S), 1.2 (l=P), and 1.6 for (l=D). Hydrogen was described by a local pseudopotential. For nitrogen and carbon S and P, for sulfur, phosphorus, and ruthenium S, P, and D angular momentum functions were included. The highest angular momentum channels were used as local potentials.

In general, the Kleinmann–Bylander scheme[70] was applied, except in the case of ruthenium where a Gauss–Hermite integration Scheme with 20 integration points was employed. Ground and excited states were described using the BP86 functional. To enable the study of isolated systems, the inherent periodicity in the plane-wave calculations was avoided by solving Poisson's equation with non-periodic boundary conditions.[71] To optimize the wave function we employed the "preconditioned conjugate gradients" method with convergence criteria of $10^{-6}$ and $10^{-3}$ for the largest element of the gradient of the wave function and for the ions, respectively. The cell size was set to $25 \times 18.75 \times 18.75$ Å$^3$, which was sufficient to converge the energies and geometries with respect to the cell parameters ($20 \times 15 \times 15$ and $24 \times 18 \times 18$ box Å$^3$ sizes were also tested).

## Structures, Energetics, and Qualitative Analysis of Photochemical Excitations of **1** and **2**

The structures of **1** and **2** were optimized in $C_i$ symmetry and are given for ruthenium as the central metal atoms in Figures 4 and 5. Structures **1a/2H$^+$** and **2a/2H$^+$** were obtained by di-protonation of **1a** and **2a** at two sulfur atoms of the ligand sphere. The complexes **1b** and **2b** were produced from **1a** and **2a**, respectively, by exchanging the orbital occupation: the $a_u$-symmetric HOMOs were depopulated and the $a_g$-symmetric LUMOs occupied by two electrons. This new electronic configuration can be understood as a model for the excited state of each of the complexes. Wavefunction and structure optimization are possible since the new occupation is kept during the self-consistent field calculations for symmetry reasons. We should note that the occupation of the LUMO within our restricted DFT calculations would imply a large contribution of a double-excited determinant in a more accurate ab initio treatment with multi-configuration wavefunctions. The inversion of HOMO–LUMO occupation should not be mixed up with an "excitation of two electrons" as one might be tempted to deduce from the qualitative picture. Moreover, the qualitative features of the "excitated" states to be discussed in this Section showed also up in *unrestricted* DFT calculations on the singlet and on the triplet (compare Section on Protonation and Reduction) states, in which only one electron is promoted from the HOMO to the LUMO (within $C_i$ symmetry).

We are aware that this procedure does not describe a stationary molecular state. However, the result of this optimization turned out to be in qualitative agreement with the more elaborate rigorous optimization techniques for excited states, which are described below. Moreover, the resulting structure provides a one-dimensional reaction coordinate, which we have also investigated by means of high-level single-point MR-MP2 techniques for excited state calculations. These test calculations confirmed the qualitative picture of the potential energy surface depicted in Figure 1.

The main contributions to the $a_g$-symmetric LUMOs in both complexes **1** and **2** are due to atomic orbitals at the ruthenium centers, at the sulfur atoms, and at the $N_2$ ligand. The contribution of the $N_2$ ligand is an antibonding π* orbital. The results of the structure optimization of the LUMO-occupied electronic configurations are depicted in the second rows of Figures 4 and 5. Their main structural feature is a bent *diazenoid* $N_2$ ligand with increased N–N bond length. In this qualitative picture, occupation of the LUMOs, which may be achieved in practice by photochemical excitation or by reduction, has thus a well-directed destabilizing effect on the $N_2$ ligand.

Since the LUMOs of $\mathbf{1a/2H^+}$ and $\mathbf{2a/2H^+}$ are qualitatively equivalent to the LUMOs of the unprotonated species, it is not surprising that exchange of occupation also yields diazenoid structures, labelled as $\mathbf{1a/2H^+}$ and $\mathbf{2a/2H^+}$ in Figures 4 and 5. The reign of the LUMO, which consists in essential parts of the antibonding π* N=N molecular orbital, attributes a certain universal character to the postulated photochemical activation process and indicates that it is indeed possible to follow different reduction routes according to Figure 2.

In Figure 4, two bond lengths of the experimentally known derivative of complex **1a** are given for comparison. As can be understood from this comparison, the B3LYP and B3LYP* calculations provide structural parameters which are in close agreement with the experimental values.

It is important to note that the slight bending of the linear $N_2$ moiety in the experimentally known dinuclear ruthenium complex is also observed for our ruthenium model complex with R = H and R′ = H. The X-ray structure features a Ru-N-N angle of 173.2°, where our model complex exhibits a corresponding angle of about 178°. This structural feature can be understood as a beginning activation of $N_2$, which is discussed from the point of view of its electronic structure in the next Section. The initial bending of $N_2$ in the dinuclear ruthenium complex in the experimental X-ray structure thus does not appear to be an artifact due to steric hindrance or packing effects in the crystal because the angle of less than 180° is also found in our simplified and isolated model complex, which we obtained from structure optimizations with tight termination criteria. In case of the **2a** complex we found a smaller bending by less than 1° (BP86/RI/TZVP).

The bond lengths of the linear $N_2$ ligands in **1a** and **2a** are only slightly increased upon coordination when compared with the free ligand (110.4 pm with BP86/RI/TZVP). $N_2$ is thus activated by the ruthenium metal centers only to a small extent. This is also evident from the N≡N stretching frequencies (BP86/RI/TZVP) of 2102 $cm^{-1}$ for complex **1a**, which is the (*R*,*S*)-stereoisomer of the experimentally known (*S*,*S*)-complex with R = P*i*Pr$_3$ and R′ = Me with $\tilde{\nu}_{N\equiv N}$ = 2047 $cm^{-1}$ (solid state).[44] The mononuclear analogue of **1a** exhibits a N–N stretching frequency of $\tilde{\nu}_{N\equiv N}$ = 2113 $cm^{-1}$.[43] For complex **2a** we obtained $\tilde{\nu}_{N\equiv N}$ = 2134 $cm^{-1}$. The decrease in wavelength by 32 $cm^{-1}$ (**1a** compared with **2a**) may be interpreted as an increased activation of $N_2$ in **1a**, which is paralleled by the stronger bending of the $N_2$ moiety. Note that the free $N_2$ ligand possesses a harmonic BP86/RI/TZVP vibrational frequency of 2361.3 $cm^{-1}$, while we obtained 1592.6 $cm^{-1}$ for the N=N stretching mode in free $N_2H_2$ (BP86/RI/TZVP). The minimum structures of the dinuclear *diazene* complexes, which are the final product of the protonation–reduction sequences, were already discussed and compared with experimental data in ref. [42].

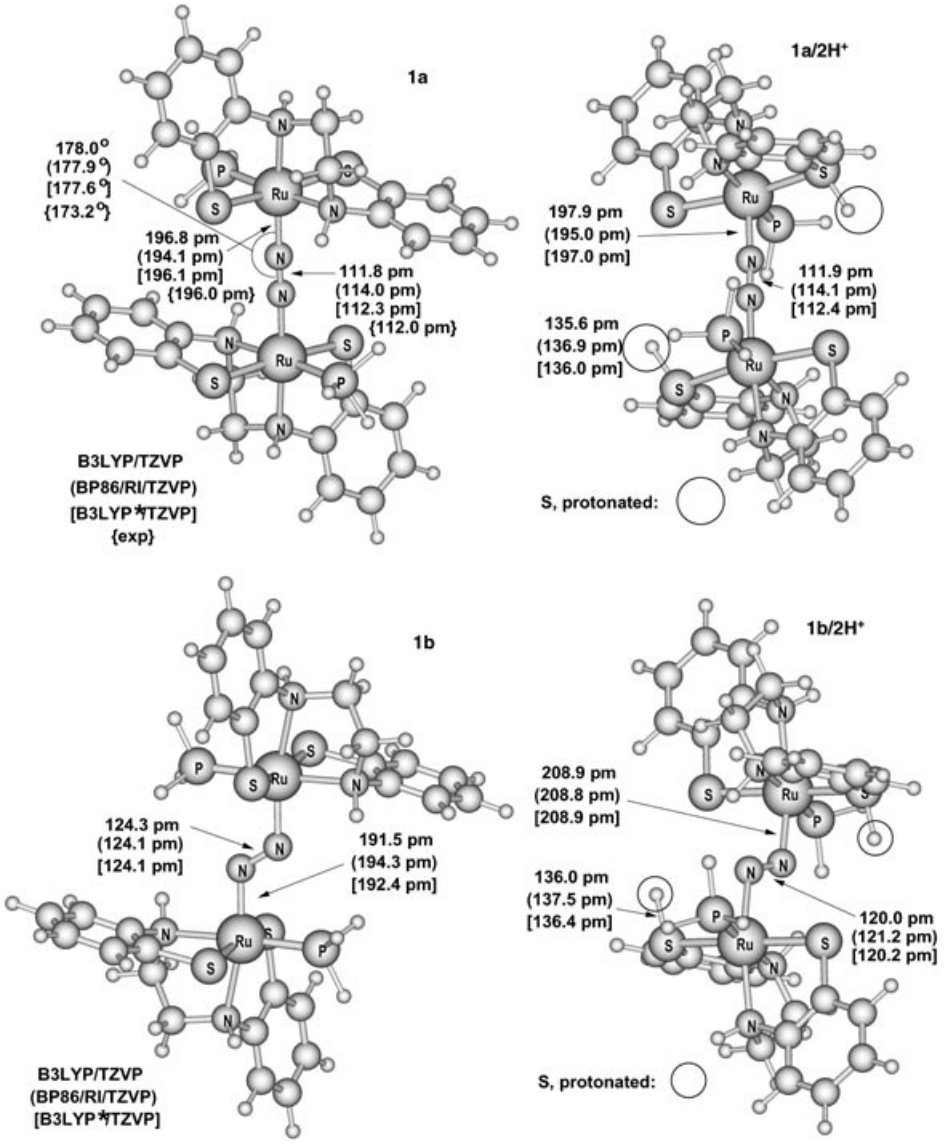


Figure 4. Optimized structures of the biomimetic model complexes **1**: ground state minimum (left), optimized structure of the HOMO–-LUMO-exchanged electronic configuration within $C_i$ symmetry (right). The top row shows the neutral ruthenium complexes and the second row depicts the positively charged complexes, where two protons were added to thiolate sulfur atoms. For **1a** experimental reference values are taken from ref. [44] for the derivative with R = P*i*Pr$_3$ and R′ = Me.

  

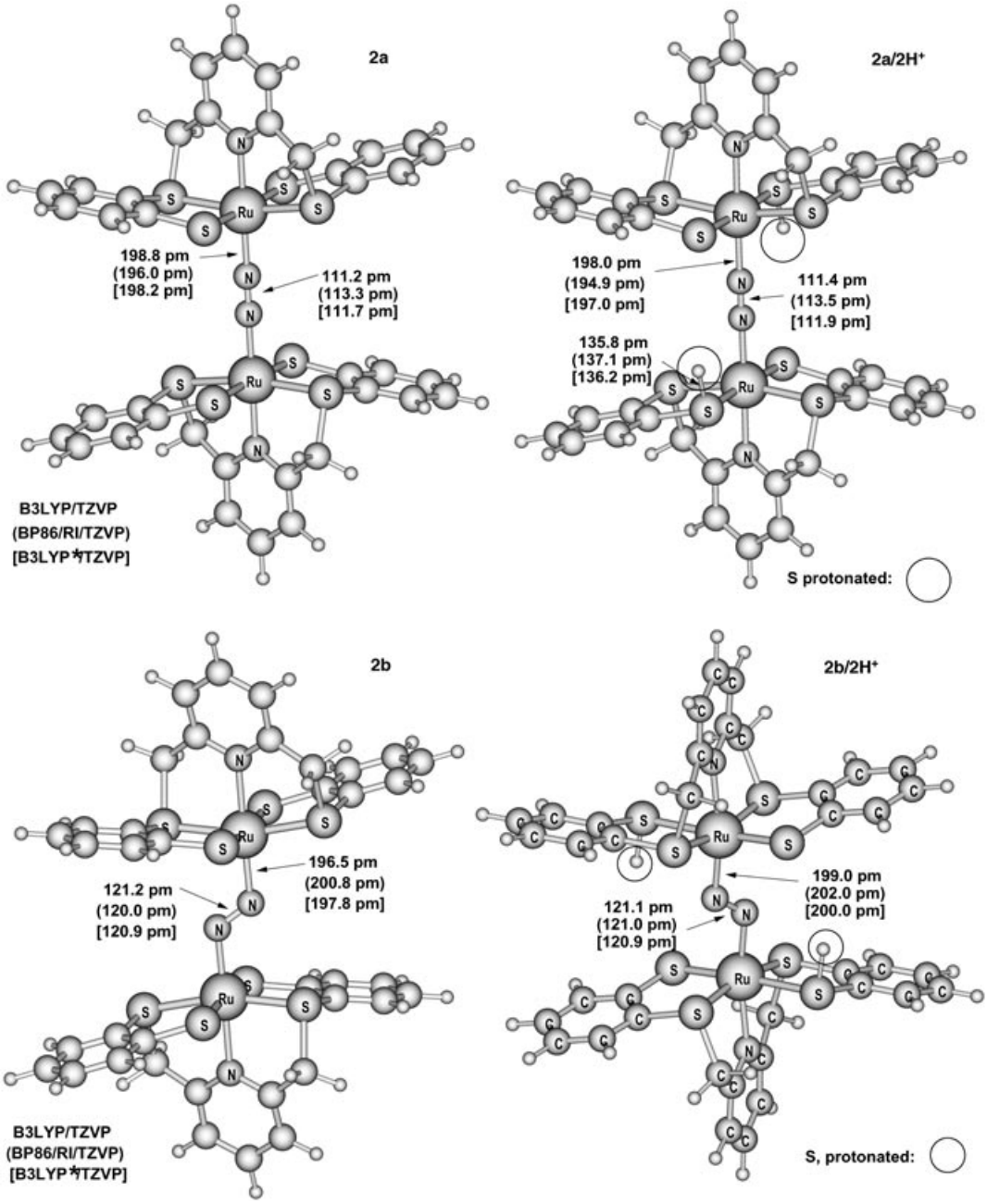


Figure 5. Optimized structures of the biomimetic model complexes **2**: ground state minimum (left), optimized structure of the HOMO–-LUMO exchanged electronic configuration within $C_i$ symmetry (right). The top row shows the neutral ruthenium complexes and the second row depicts the positively charged complexes, where two protons were added to thiolate sulfur atoms.

The corresponding dinuclear $N_2$-coordinating $Fe^{II}$ complexes exhibit the same structural features as the dinuclear ruthenium complexes and behave analogously with respect to a re-occupation of molecular orbitals. The **1(Fe)a** complex also exhibits a initial bending of the Fe-N≡N-Fe moiety with an Fe-N-N angle of 177.3°. The analogous behaviour of the dinuclear $Fe^{II}$ and $Ru^{II}$ complexes adds to the universal character of the photochemical activation process. Since to date only the dinuclear dinitrogen complex **1** with ruthenium as the central metal is known, we restrict the following discussion to the ruthenium complexes for brevity.

Energetics for various reactions of the complexes **1** and **2** are listed in Table 1 in order to provide qualitative insight into the relative energies of the different species. Reaction type (A), which is endothermic by 41.1 kJ mol$^{-1}$ for **1a** and by 18.6 kJ mol$^{-1}$ for **2a**, produces the corresponding diazene complexes **3** and **4**, respectively. The excitation energies of about 3.5 eV for reactions (B.a) and (B.b) in Table 1 are only rough estimates for the true values (in view of the somewhat artificial generation of the diazenoid structures by inversion of the HOMO–LUMO occupation).

Table 1. Reaction energetics of complexes **1** and **2** at 0 K (without zero-point energy corrections) within the semi-quantitative approach [kJ mol$^{-1}$].

| type | Reaction reactants | BP86/RI TZVP | B3LYP TZVP | B3LYP* TZVP |
|---|---|---|---|---|
| (A) | **1a**+$H_2$→**3** | 29.1 | 45.1 | 41.1 |
| (B.a) | **1a**→**1b** | 244.2 | 310.1 | 292.2 |
| (B.b) | **1a/2H$^+$**→**1b/2H$^+$** | 312.3 | 387.1 | 366.5 |
| (A) | **2a**+$H_2$→**4** | 5.0 | 23.4 | 18.6 |
| (B.a) | **2a**→**2b** | 286.6 | 362.3 | 343.0 |
| (B.b) | **2a/2H$^+$**→**2b/2H$^+$** | 310.0 | 384.9 | 364.3 |

## Quantitative Investigation into the Excitation and Relaxation Processes

In the last Section, we described general evidence for a possible photoexcitation of complexes **1** and **2**, which can yield diazenoid structures with activated $N_2$ moieties ready to be (protonated and) reduced. Our discussion so far was based on calculations of excited states in which we assumed that the excited state wave function is qualitatively well described by a point-group-restricted DFT optimization within $C_i$ symmetry.

For a quantitative study in a TDDFT and MR-MP2 framework, we used a modified model **5** of the experimentally known dinuclear ruthenium complex **1** in order to increase the computational efficiency. We should note that this reduced model, in which the benzene rings have been substituted by ethylene bridges, also shows the general qualitative properties of the dinuclear complexes **1** and **2**, that is, it also bends upon exchange of HOMO and LUMO occupation (see Figure 6).

A TDDFT geometry optimization of **5a** in its first excited singlet state gave an asymmetrically bent species **5b**, which is depicted in Figure 7. In the qualitative test calculations with exchanged occupation in $C_i$ symmetry we found bending angles of about 120°, while the Ru-N-N angles in the TDDFT $S_1$-optimized structure **3b** are 138.3 and 147.0°. The consistent picture of TDDFT excited state structure optimization thus corroborates evidence that a photochemical activation of $N_2$ is possible, if the LUMO is governed by π* contributions of the $N_2$ ligand.

As in the case of the "full" complexes **1a** and **2a**, also **5a** shows a characteristic LUMO with an antibonding contribution at the $N_2$ ligand. This LUMO is shown in Figure 8.

It is instructive to use the electron localization function (ELF)[72] as a means for the analysis of the total electronic density. Since ELF is a measure for the probability of finding a second electron at the position of a given one, visualization of electron lone pairs is possible. ELF isosurfaces and conture plots for the model complex **2** are given in Figure 9.

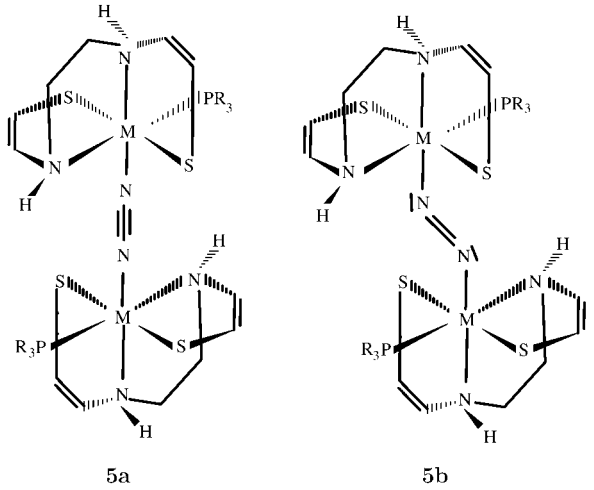


Figure 6. Lewis structures of the ruthenium-based model system **5**.

ELF reveals tiny lone pairs at the nitrogen atoms of the slightly bent $N_2$ ligand in **5a**. This initial formation of lone pairs is the electronic signature of the structural distortion from linearity. In the diazenoid structure **5b** in Figure 9, the lone pairs are, as expected, much more pronounced and may function as acceptors for protons near-by.

Since it was not possible to obtain reliable excitation energies with TDDFT for the structures **5a** and **5b**, we used the more accurate MR-MP2 theory for this purpose. The BP86 and B3LYP $S_0 \rightarrow S_1$ excitation energies differed by about 0.5 eV and were both smaller than 2.0 eV.

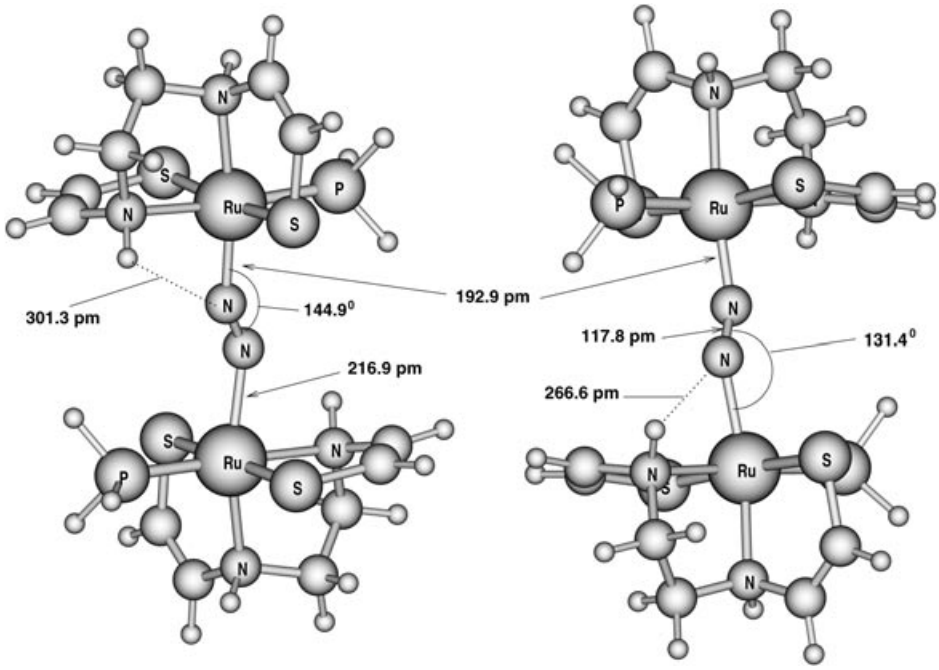


Figure 7. Two different views upon the BP86–plane-wave optimized structure of the first-excited $S_1$ state of the ruthenium-based model system **5b**.

  

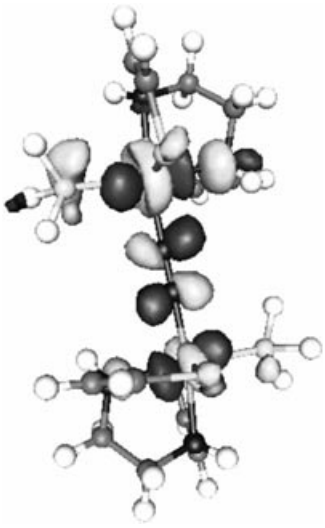

Figure 8. LUMO of the linear structure of model complex **5a**.

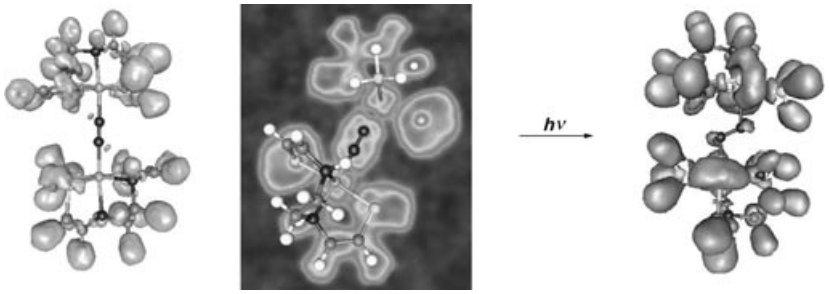


Figure 9. ELF plots of structures **3a** and **3b** before and after the excitation. The linear structure on the left and in the middle is depicted with an ELF isosurface at 0.76 and as a contour plot, respectively. The bent structure on the right shows ELF at a value of 0.85. (The specific values for the ELF isosurface have been selected for practical purposes.) The left-hand-side plot shows a very small lone pair, which originates from the slight distortion of the linear minimum structure. The picture in the middle clearly shows the lone pairs at the sulfur atoms, which are the protonation positions. The right-hand plot demonstrates the rise of lone pairs in the diazenoid bent structure.

It is important to note that the structure of the multi-determinant wave function of **5a** shows a significant contribution from $\pi^2 \rightarrow \pi^{*2}$ *doubly* excited determinants (the Hartree-Fock ground state wave function has a configuration interaction (CI) weight of $C^2_{\mathrm{HF}} = 0.80$), as we would have expected from the qualitative discussion in the Section on the Structures, Energetics, and Qualitative Analysis. This observation correlates with the deviation of the Ru-N≡N moiety from linearity by about 3°. On the other hand, the excited state wave function of **5b** is dominated by a contribution from a HOMO→LUMO single excitation with a CI weight of $C^2_{\mathrm{HOMO}\rightarrow\mathrm{LUMO}} = 0.60$.

After testing various reference configurations in the MR-MP2 protocol, we obtained two optimum results for the ground and excited-state energies. By comparison of total electronic energies, the first calculation gave a better description of the excited state ($E_{S_0} = -3257.759242$ Hartree, $E_{S_1} = -3257.573900$ Hartree), while the second calculation revealed an optimum description of the ground state ($E_{S_0} = -3257.775261$ Hartree, $E_{S_1} = -3257.561907$ Hartree). From both MR-MP2 calculations for the linear $N_2$ complex we take the lowest energies for the ground state and for the first excited singlet state. The vertical excitation energy of **5a** then becomes 5.48 eV (226 nm). If this energy can be selectively deposited in **5a**, the structure may relax to **5b**, for which we find a "de-excitation" energy of 1.75 eV (711 nm). The relaxation in the first excited $S_1$ state thus produces the diazenoid structure and reduces the electronic gap between the $S_0$ and $S_1$ states as suggested by Figure 1.

## Protonation and Reduction of the Excited-State Minimum Structures

Following the upper reaction pathway of Figure 2, we may model the last two steps, that is, the protonation and reduction, *at once* by adding two hydrogen atoms to the thiolate sulfur atoms in the $S_1$-minimum structure at distances and angles, which are typical for *protons* bound to thiolate sulfurs in such complexes (i.e., at $d$(S–H) = 137 pm, $a$(RuSH) = 100°, and $d$(NRuSH) = −10°). To model the transfer of hydrogen atoms onto the diazenoid structure in a simple way, we relaxed the thus prepared structure **5b**+2H in a standard ground state structure optimization. However, since four sulfur atoms in **5b** approximately span a plane, in which the two metal atoms as well as the $N_2$ ligand lies, there exist two possibilities to efficiently protonate a *trans*-pair of sulfur atoms (other protonation schemes are also possible but less effective with respect to $N_2$ reduction). Both possibilities may yield two different diazene isomers (compare refs. [73–76] complexes) depending on the pre-orientation of the bent-$N_2$ moiety with respect to the plane of the four sulfur atoms. This pre-orientation is determined by the chelate ligand because the bent-$N_2$ ligand minimizes the lone-pair-lone-pair repulsion with the sulfur atoms.

In the case of **5b**+2H, our first di-protonation and reduction attempt did not produce spontaneously the diazene complex. This is an indication for the occurrence of a small barrier, which could not be overcome in the structure optimization process (a molecular dynamics treatment at finite temperature would be more appropriate for this purpose). However, starting from a di-protonation plus reduction of the second *trans*-pair of sulfur atoms did indeed show spontaneous reduction of the bent-$N_2$ complex **5b** and the dinuclear diazene complex was obtained. We should note that it is not possible to investigate the dependence of the H transfer efficiency on the RuNN (bending) angle, because di-electron-reduction always yields the diazene complex even in those cases for which the RuNN angle is close to 180°; the complex then follows the lower pathway of Figure 2.

The first time, we observed spontaneous hydrogen atom transfer after di-protonation of different sulfur *trans*-pairs was for a derivative **6b** of complex **2b** (see Figure 10). In the case of these [M"$N_xS_4$"]$_2$L-type complexes we have two vertical "$S_4$" planes and thus at least four sulfur *trans*-pairs. The BP86 optimized structures of the linear ground state of one of the di-protonated isomers of the $Fe^{II}$ complex **6a** and of the corresponding protonated diazenoid system **6b/2H$^+$** are depicted in Figure 10. Structure **6b/2H$^+$** was generated by optimization of the exchanged HOMO–LUMO configuration. Upon two-electron reduction of **6b/2H$^+$** we found spontaneous hydrogen atom transfer onto the diazenoid $N_2$ moiety and obtained the diazene complex. Note that the $N_2$ complex **6a** is neither with $Fe^{II}$ nor with $Ru^{II}$ centers known; the corresponding iron diazene complex was, however, synthesized with $Fe^{II}$ centers.[50]

The different relaxation behavior of **6b**+2H when compared with the "$N_2S_2$" series of complexes **1** and **5** can be explained in terms of the particular structural features of **6b/2H$^+$**: the acceptor lone pairs at the diazenoid moiety point into the direction of the protons bound to the sulfur atoms. This differs from what we find for **1b/2H$^+$** and **5b/2H$^+$**, where the plane of diazenoid $N_2$ is rotated farther away from the protons at the sulfur atoms. Consequently, a reduction of diazenoid $N_2$ requires first an into-plane rotation, which is affected by an activation barrier. This barrier can prevent spontaneous hydrogen atom transfer in the cases of **1b/2H$^+$** and **5b/2H$^+$**. Since the alignment of the diazenoid-$N_2$ plane is determined by the interaction of this moiety with atoms from the chelate ligand (for instance, by repulsion of nitrogen and sulfur lone pairs), the complexes under study show a nice example of reactivity control through secondary ligand effects.

Finally, we should note that it is possible to generate a diazenoid $N_2$ complex by excitation into the lowest-lying triplet state $T_1$. This state can be described by standard Kohn-Sham DFT methods and can thus be optimized in a standard DFT calculation. Optimizing a triplet state of the dinuclear complexes under consideration requires the single occupation of the $\pi^*$-antibonding LUMO, which is the reason for the bending of $N_2$ in the $T_1$ state, which we observed. Owing to this principle, we were also able to optimize a di-protonated *diazenoid* complex in the triplet state. These observations for the $T_1$ state confirm the universal character of the $N_2$ activation Scheme and point to an additional possibility to prepare excited-state diazenoid $N_2$ complexes ready for reduction. Moreover, the di-protonated triplet structures may be used as models for the di-protonated diazenoid singlet structures, which are only accessible via very computer-time demanding excited-state structure optimizations.

Our results for the modeling of hydrogen atom transfer are a strong indication that the proposed photochemical activation and protonation/reduction of $N_2$ is feasible and, secondly, a universal feature of dinuclear $Fe^{II}$- and $Ru^{II}$–sulfur complexes.

## Conclusion

We have studied a general photochemical activation process for inert dinitrogen bound to the two metal centers ruthenium(II) or iron(II). The universal character of this process is manifest in the one-particle interpretation of the electronic excitation: upon vertical excitation into an antibonding $\pi^*$ orbital the $N_2$ triple bond is weakened. This allows for a relaxation of the excited complex towards a bent, diazene-like $N_2$ moiety. This diazenoid excited-state complex is then prepared for a take up of protons and electrons to give diazene. However, the protons could have been delivered prior to photochemical activation and subsequent reduction.

For this process, it is essential to bind $N_2$ to two metal centers since the identification of a diazenoid species rests upon the preferential orientation induced through coordination of $N_2$. In other words, only coordinated dinitrogen is able to exhibit a lone pair per nitrogen atom since the linear symmetry of the free $N_2$ is broken by the metal centers bound to each nitrogen atom.

A feature of the universal character of the excitation process is the ability to bind protons to the sulfur atoms in the ligand spheres of the complexes. In the one-particle picture of qualitative molecular orbital theory, this protonation involves molecular orbitals mainly generated by sulfur atomic orbitals, while the LUMO remains to be the one, which describes the antibonding $\pi^*$ situation of the $N_2$ ligand clamped between the two metal centers. Consequently, the electronic excitation from HOMO to LUMO involves the same type of orbitals as in the unprotonated species and the diazenoid structure results after structural relaxation in the first excited state.

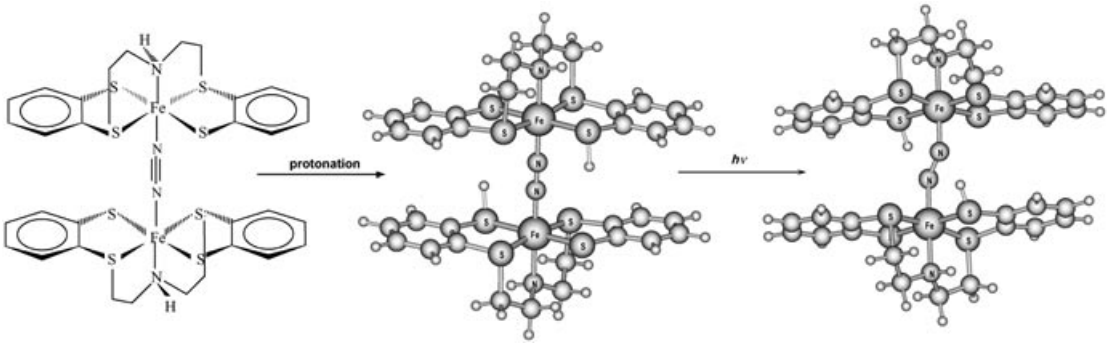


Figure 10. BP86 optimized structure of the doubly protonated linear complex **6a/2H$^+$** and resulting structure **6b/2H$^+$** after optimization with exchange of HOMO–LUMO occupation.

  

First experimental reduction as well as photochemical irradiation experiments of **1** are currently being studied.[77] The experimental realization is, however, not a trivial task since side reactions have to be suppressed. For instance, protonation attempts of the particular coordinatination sphere of **1** show a weakening of the coordination of dinitrogen.[77] In order to strengthen the coordination of dinitrogen, tuning via secondary effects of the molecular chelate ligand architecture (e.g., by introducing a bidentate phosphine, which clamps the two metal fragments) might be useful (see also the work of other groups[12,13]). Possible occurrence of dinitrogen loss in experimental set ups through irradiation into a repulsive, higher excited state, has also been observed for dinitrogen complexes and might become a side reaction, too; see, for instance, refs. [78,79] for a mechanistic study on photochemically induced $N_2$ loss from *trans*-$[(N_2)_2W(dppe)_2]$ with dppe = 1,2-bis-diphenylphosphinoethane); the excited states of this complex were later assigned by Brummer and Crosby.[80] Such side processes might be overcome by the use of a tailored laser wavelength in order to exactly meet the excitation energy for the $S_0 \rightarrow S_1$ transition.

To conclude, we have presented a detailed theoretical study of various aspects of a postulated universal activation principle of $N_2$, which involved the investigation of the possible sequences of activation, protonation, and reduction steps for two different metal centers in various chelate ligand environments (all carrying sulfur donor atoms in order to allow for binding of protons) and different electronically excited states (namely the first excited singlet and triplet states). This activation Scheme should provide a feasible route to dinitrogen activation and reduction if the LUMO is governed by the $\pi^*$-antibonding orbital of the $N_2$ ligand.

## Acknowledgement

The authors would like to thank Prof. H. Kisch for valuable discussions. This work was financially supported by the Collaborative Research Center SFB 583 "Redoxaktive Metallkomplexe" and by the Fonds der Chemischen Industrie. J.H. thanks the Swiss national science foundation (SNF 200020-100417) and B.K. would like to acknowledge support by the Deutsche Forschungsgemeinschaft DFG and by a Forschungskredit of the Universität Zürich. The excited state structure optimizations were carried out at the Rechenzentrum Garching of the Max-Planck-Institut für Plasmaphysik within the framework of the project h023z at the supercomputing center Bavaria (HLRB).

[1] W. J. Evans, G. Zucchi, J. W. Ziller, *J. Am. Chem. Soc.* **2003**, *125*, 10–11.
[2] M. D. Fryzuk, B. A. MacKay, B. O. Patrick, *J. Am. Chem. Soc.* **2003** *125*, 3234–3235.
[3] J. Chatt, J. R. Dilworth, R. L. Richards, *Chem. Rev.* **1978** *78*, 589–625.
[4] R. A. Henderson, G. J. Leigh, C. J. Pickett, *Adv. Inorg. Chem. Radiochem.* **1983**, *27*, 198–292.
[5] M. Hidai, Y. Mizobe, *Chem. Rev.* **1995**, *95*, 1115–1133.
[6] M. D. Fryzuk, S. A. Johnson, *Coord. Chem. Rev.* **2000**, *200–202*, 379–409.
[7] J. Chatt, A. J. Pearman, R. L. Richards, *J. Chem. Soc. Dalton Trans.* **1976**, 1520.
[8] M. Hidai, T. Kodama, M. Sato, M. Harakawa, Y. Uchida, *Inorg. Chem.* **1976**, *15*, 2694–2697.
[9] J. P. Collman, J. E. Hutchison, M. A. Lopez, R. Guilard, R. A. Reed, *J. Am. Chem. Soc.* **1991**, *113*, 2794–2796.
[10] J. P. Collman, J. E. Hutchison, M. S. Ennis, M. A. Lopez, R. Guilard, *J. Am. Chem. Soc.* **1992**, *114*, 8074–8080.
[11] J. P. Collman, J. E. Hutchison, M. A. Lopez, R. Guilard, *J. Am. Chem. Soc.* **1992**, *114*, 8066–8073.
[12] Y. Nishibayashi, S. Iwai, M. Hidai, *Science* **1998**, *279*, 540–542.
[13] Y. Nishibayashi, I. Wakiji, K. Hirata, M. R. D. Bois, M. Hidai, *Inorg. Chem.* **2001**, *40*, 578–580.
[14] J. M. Smith, R. J. Lachicotte, K. A. Pittard, T. R. Cundari, G. Lukat-Rodgers, K. R. Rodgers, P. L. Holland, *J. Am. Chem. Soc.* **2001**, *123*, 9222–9223.
[15] S. M. P. R. M. Cunha, M. F. C. G. da Silva, A. J. L. Pombeiro, *Inorg. Chem.* **2003**, *42*, 2157–2164.
[16] E. Solari, C. D. Silva, B. Iacono, J. Hesschenbrouck, C. Rizzoli, R. Scopelliti, C. Floriani, *Angew. Chem.* **2001**, *113*, 4025–4027; *Angew. Chem. Int. Ed.* **2001**, *40*, 3907–3909.
[17] G. N. Schrauzer, T. D. Guth, *J. Am. Chem. Soc.* **1977**, *99*, 7189–7193.
[18] O. Rusina, A. Eremenko, G. Frank, H. P. Strunk, H. Kisch, *Angew. Chem.* **2001**, *113*, 4115–4117; *Angew. Chem. Int. Ed.* **2001**, *40*, 3993–3995.
[19] O. Rusina, O. Linnik, A. Eremenko, H. Kisch, *Chem. Eur. J.* **2003**, *9*, 561–565.
[20] D. L. Boucher, J. A. Davies, J. G. Edwards, A. Mennad, *J. Photochem. Photobiol. A* **1995**, *88*, 53–64.
[21] J. G. Edwards, J. A. Davies, D. L. Boucher, A. Mennad, *Angew. Chem.* **1992**, *104*, 489; *Angew. Chem. Int. Ed. Engl.* **1992**, *31*, 480.
[22] S. Sekusak, G. Frenking, *J. Mol. Struct. (Theochem)* **2001**, *541*, 17–29.
[23] G. N. Schrauzer, *Angew. Chem.* **1975**, *87*, 579–587; *Angew. Chem. Int. Ed.* **1975**, *14*, 514.
[24] E. I. Stiefel, The Mechanism of Nitrogen Fixation in *Recent Developments in Nitrogen Fixation* (Eds.: W. Newton, J. R. Postgate, C. Rodriguez-Barrueco), Academic Press, London, **1977**.
[25] B. K. Burgess, D. J. Lowe, *Chem. Rev.* **1996**, *96*, 2983–3012.
[26] R. R. Eady, *Chem. Rev.* **1996**, *96*, 3013–3030.
[27] J. B. Howard, D. C. Rees, *Chem. Rev.* **1996**, *96*, 2965–2982.
[28] D. V. Yandulov, R. R. Schrock, *J. Am. Chem. Soc.* **2002**, *124*, 6252–6253.
[29] D. V. Yandulov, R. R. Schrock, *Science* **2003**, *301*, 76–78.
[30] R. R. Schrock, *Chem. Commun.* **2003**, 238–239.
[31] I. Fischer, E. K. von Gustorf, *Naturwissenschaften* **1975**, *62*, 63–70.
[32] I. M. Treitel, M. T. Flood, R. E. Marsh, H. B. Gray, *J. Am. Chem. Soc.* **1969**, *91*, 6512–6513.
[33] A. D. Allen, J. R. Stevens, *Can. J. Chem.* **1972**, *50*, 3093–3099.
[34] A. B. P. Lever, G. A. Ozin, *Inorg. Chem.* **1977**, *16*, 2012–2016.
[35] R. O. Louro, T. Catarino, J. LeGall, D. L. Turner, A. V. Xavier, *ChemBioChem* **2001**, *2*, 831–837.
[36] D. Sellmann, J. Sutter, *J. Biol. Inorg. Chem.* **1996**, *1*, 587–593.
[37] D. Sellmann, J. Sutter, *Acc. Chem. Res.* **1997**, *30*, 460–469.
[38] D. Sellmann, J. Utz, N. Blum, F. W. Heinemann, *Coord. Chem. Rev.* **1999**, *190–192*, 607–627.
[39] D. Sellmann, J. Sutter, "Biological $N_2$ fixation: Molecular mechanism of the nitrogenase catalyzed $N_2$ dependent HD formation, the $N_2$ fixation inhibition and the open-side FeMoco model, in Perspectives in Coordination Chemistry (Eds.: A. M. Trzeciak, P. Sobota, J. J. Ziolkowski), *Education on Advanced Chemistry*, *Vol. 7*, University of Wroclaw, Poland, **2000**, pp. 49–65.
[40] D. Sellmann, A. Fürsattel, J. Sutter, *Coord. Chem. Rev.* **2000**, *200–202*, 541–561.
[41] J. Schimpl, H. M. Petrilli, P. E. Blöchl, *J. Am. Chem. Soc.* **2003**, *125*, 15772–15778.
[42] M. Reiher, O. Salomon, D. Sellmann, B. A. Hess, *Chem. Eur. J.* **2001**, *7*, 5195–5202.
[43] D. Sellmann, B. Hautsch, A. Rösler, F. W. Heinemann, *Angew. Chem.* **2001**, *113*, 1553–1558; *Angew. Chem. Int. Ed.* **2001**, *40*, 1505–1507.
[44] D. Sellmann, A. Hille, F. W. Heinemann, M. Moll, A. Rösler, J. Sutter, G. Brehm, M. Reiher, B. A. Hess, S. Schneider, *Inorg. Chim. Acta* **2003**, *348*, 194–198.

  

[45] D. Sellmann, A. Hille, A. Rösler, F. W. Heinemann, M. Moll, G. Brehm, S. Schneider, M. Reiher, B. A. Hess, W. Bauer, *Chem. Eur. J.* **2004**, *10*, 819 – 830.
[46] D. Sellmann, J. Utz, F. W. Heinemann, *Inorg. Chem.* **1999**, *38*, 5314 – 5322.
[47] D. Sellmann, K. Engl, F. W. Heinemann, *Eur. J. Inorg. Chem.* **2000**, 423 – 429.
[48] D. Sellmann, D. Häußinger, T. Gottschalk-Gaudig, F. W. Heinemann, *Z. Naturforsch.* **2000**, *55b*, 723 – 729.
[49] D. Sellmann, N. Blum, F. W. Heinemann, *Z. Naturforsch.* **2001**, *56b*, 581 – 588.
[50] D. Sellmann, W. Soglowek, F. Knoch, M. Moll, *Angew. Chem.* **1989**, *101*, 1244 – 1245; *Angew. Chem. Int. Ed. Engl.* **1989**, *28*, 1271 – 1272.
[51] R. Ahlrichs, M. Bär, M. Häser, H. Horn, C. Kölmel, *Chem. Phys. Lett.* **1989**, *162*, 165 – 169.
[52] D. Andrae, U. Häußermann, M. Dolg, H. Stoll, H. Preuß, *Theor. Chim. Acta* **1990**, *77*, 123 – 141.
[53] A. Schäfer, C. Huber, R. Ahlrichs, *J. Chem. Phys.* **1994**, *100*, 5829.
[54] A. D. Becke, *Phys. Rev. A* **1988**, *38*, 3098 – 3100.
[55] J. P. Perdew, *Phys. Rev. B* **1986**, *33*, 8822 – 8824.
[56] A. D. Becke, *J. Chem. Phys.* **1993**, *98*, 5648 – 5652.
[57] P. J. Stephens, F. J. Devlin, C. F. Chabalowski, M. J. Frisch, *J. Phys. Chem.* **1994**, *98*, 11 623 – 11 627.
[58] R. Bauernschmitt, R. Ahlrichs, *J. Chem. Phys.* **1996**, *104*, 9047 – 9052.
[59] R. Bauernschmitt, M. Häser, O. Treutler, R. Ahlrichs, *Chem. Phys. Lett.* **1997**, *264*, 573 – 578.
[60] R. Bauernschmitt, R. Ahlrichs, *Chem. Phys. Lett.* **1996**, *256*, 454 – 464.
[61] K. Eichkorn, O. Treutler, H. Öhm, M. Häser, R. Ahlrichs, *Chem. Phys. Lett.* **1995**, *240*, 283 – 290.
[62] K. Eichkorn, F. Weigend, O. Treutler, R. Ahlrichs, *Theor. Chem. Acc.* **1997**, *97*, 119 – 124.
[63] M. Reiher, O. Salomon, B. A. Hess, *Theor. Chem. Acc.* **2001**, *107*, 48 – 55.
[64] O. Salomon, M. Reiher, B. A. Hess, *J. Chem. Phys.* **2002**, *117*, 4729 – 4737.
[65] J. Neugebauer, M. Reiher, C. Kind, B. A. Hess, *J. Comput. Chem.* **2002**, *23*, 895 – 910.
[66] S. Grimme, M. Waletzke, *Phys. Chem. Chem. Phys.* **2000**, *2*, 2075 – 2081.
[67] J. Hutter, *J. Chem. Phys.* **2003**, *118*, 3928 – 3934.
[68] CPMD V3.6, http://www.cpmd.org, Copyright IBM Corp. 1995–2002; Copyright MPI für Festkörperforschung Stuttgart 1997–2001, Zürich, **2002**.
[69] N. Troullier, J. L. Martins, *Phys. Rev. B* **1991**, *43*, 1993 – 2006.
[70] L. Kleinmann, D. M. Bylander, *Phys. Rev. Lett.* **1982**, *48*, 1425 – 1428.
[71] G. J. Martyna, M. E. Tuckerman, *J. Chem. Phys.* **1999**, *110*, 2810 – 2821.
[72] A. D. Becke, K. E. Edgecombe, *J. Chem. Phys.* **1990**, *92*, 5397 – 5403.
[73] N. Lehnert, B. E. Wiesler, F. Tuczek, A. Hennige, D. Sellmann, *J. Am. Chem. Soc.* **1997**, *119*, 8879 – 8888.
[74] D. Sellmann, D. C. F. Blum, F. W. Heinemann, *Inorg. Chim. Acta* **2002**, *337*, 1 – 10.
[75] J. Neugebauer, M. Reiher, B. A. Hess, Structure, Energetics, and Spectroscopy of Models for Enzyme Cofactors, in *High-Performance Computing in Science and Engineering 2000–2002 — Transactions of the First Joint HLRB and KONWIHR Status and Result Workshop*, Springer, Berlin, **2003**, pp. 157 – 169.
[76] M. Reiher, J. Neugebauer, B. A. Hess, *Z. Phys. Chem. (Muenchen Ger.)* **2003**, *217*, 91 – 103.
[77] D. Sellmann, A. Hille, unpublished results, University of Erlangen-Nuremberg, **2003**.
[78] A. Caruana, H. Kisch, *Angew. Chem.* **1979**, *91*, 335 – 336; *Angew. Chem. Int Ed.* **1979**, *18*, 328.
[79] A. Caruana, H. Hermann, H. Kisch, *J. Organomet. Chem.* **1980**, *187*, 349 – 359.
[80] J. G. Brummer, G. A. Crosby, *Inorg. Chem.* **1985**, *24*, 552 – 558.

Received: January 24, 2004
Published online: July 27, 2004

  